

## Mott physics in the 2*p* electron dioxygenyl magnet O<sub>2</sub>MF<sub>6</sub> (*M* = Sb, Pt)

Minjae Kim and B. I. Min

*Department of Physics, PCTP, Pohang University of Science and Technology, Pohang 790-784, Korea*

(Received 27 July 2011; published 22 August 2011)

We have investigated electronic structures and magnetic properties of O<sub>2</sub>MF<sub>6</sub> (*M* = Sb, Pt), which are composed of two building blocks of strongly correlated electrons: O<sub>2</sub><sup>+</sup> dioxygenyls and MF<sub>6</sub><sup>−</sup> octahedra, by employing the first-principles electronic structure band method. For O<sub>2</sub>SbF<sub>6</sub>, as a reference system of O<sub>2</sub>PtF<sub>6</sub>, we have shown that the Coulomb correlation of O(2*p*) electrons drives the Mott insulating state. For O<sub>2</sub>PtF<sub>6</sub>, we have demonstrated that the Mott insulating state is induced by the combined effects of the Coulomb correlation of O(2*p*) and Pt(5*d*) electrons and the spin-orbit (SO) interaction of Pt(5*d*) states. The role of the SO interaction in forming the Mott insulating state of O<sub>2</sub>PtF<sub>6</sub> is similar to the case of Sr<sub>2</sub>IrO<sub>4</sub> that is a prototype of a SO-induced Mott system with  $J_{\text{eff}} = 1/2$ .

DOI: [10.1103/PhysRevB.84.073106](https://doi.org/10.1103/PhysRevB.84.073106)

PACS number(s): 71.20.-b, 71.27.+a, 71.70.Ej, 75.50.Xx

Mott transition in strongly correlated electron systems has been extensively studied for 3*d* transition metal (TM) oxides, in which the degenerate 3*d* states are usually split by the crystal field (CF) and then the Coulomb correlation effect produces the energy separation between the upper and the lower Hubbard bands.<sup>1</sup> The spin-orbital dependent superexchange interaction of Kugel-Khomskii type can be derived based on orbital polarizations of 3*d* states in these Mott insulating states.<sup>2,3</sup> According to recent experimental and theoretical works, the similar Mott physics is realized in 2*p* electron molecular solids (KO<sub>2</sub>)<sup>4-6</sup> and also in 5*d* TM oxides (Sr<sub>2</sub>IrO<sub>4</sub>),<sup>7-10</sup> which signifies a new paradigm of spin-orbital physics. The bands in 2*p* electron molecular solids are almost like molecular levels due to the weak intermolecular interaction, and so the bandwidth *W* near the Fermi level *E<sub>F</sub>* is small with respect to on-site Coulomb repulsion *U*, resulting in the Mott insulating state.<sup>4-6</sup> On the other hand, in 5*d* TM oxides, the large spin-orbit (SO) interaction as much as ~0.4 eV (Ref. 7) brings about the small *W* by lifting the degeneracy of 5*d* states and also by reducing the hopping strength.<sup>7,10</sup> In the strong SO interaction limit, electronic structures of 5*d* TM oxides are determined by the relative magnitude between *W* and *U* of 5*d* electrons.<sup>8,9</sup> In this context, dioxygenyl magnet O<sub>2</sub>PtF<sub>6</sub> is interesting in that it is a 2*p* electron molecular solid containing a 5*d* TM element, which possesses effects of both the strong Coulomb correlation and the strong SO interaction.<sup>11-13</sup>

O<sub>2</sub>MF<sub>6</sub> (*M* = Sb, Pt) were reported to be insulators.<sup>14-16</sup> O<sub>2</sub>MF<sub>6</sub> is composed of O<sub>2</sub><sup>+</sup> dioxygenyls and MF<sub>6</sub><sup>−</sup> octahedra, as depicted in Fig. 1. Dioxygenyl O<sub>2</sub><sup>+</sup> ion has the electronic configuration of  $\sigma_g^2\pi_u^4\pi_g^{*1}$  [see Fig. 2(a)]. Hence, the localized magnetic moment would be generated from one unpaired electron on the degenerate  $\pi_g^*$  orbital. Magnetic susceptibility data showed the Curie-Weiss behaviors with low Curie temperatures,  $T_C = 0.8$  K for O<sub>2</sub>SbF<sub>6</sub> and  $T_C = 4$  K for O<sub>2</sub>PtF<sub>6</sub>, which implies the rather weak superexchange interaction between localized magnetic moments. Electron spin resonance (ESR) experiment also revealed the existence of the localized magnetic moment of O<sub>2</sub><sup>+</sup> in O<sub>2</sub>SbF<sub>6</sub> and the ferrimagnetic ordering between the magnetic moments of O<sub>2</sub><sup>+</sup> and Pt in O<sub>2</sub>PtF<sub>6</sub> (Ref. 15).

Local electronic structure of O<sub>2</sub><sup>+</sup> in Fig. 2 is similar to that of O<sub>2</sub><sup>−</sup> in KO<sub>2</sub> superoxide that has one hole (three

electrons) in the  $\pi_g^*$  state. Electronic structure calculations for various superoxides (KO<sub>2</sub>, RbO<sub>2</sub>, Rb<sub>4</sub>O<sub>6</sub>) indicated that the conventional local density approximation (LDA) or the generalized gradient approximation (GGA) underestimates the Coulomb correlation interaction of open shell 2*p* electrons in superoxides. Only after the inclusion of on-site Coulomb repulsion *U* in the LDA + *U* or GGA + *U* schemes was the insulating nature of superoxides properly described.<sup>4,5,17-21</sup>

We have investigated electronic structures and magnetic properties of O<sub>2</sub>PtF<sub>6</sub> by employing the first-principles band structure calculation incorporating both the Coulomb correlation and the SO effect. As a reference system, we have also examined electronic structures of O<sub>2</sub>SbF<sub>6</sub>. For O<sub>2</sub>SbF<sub>6</sub>, we have confirmed that the Coulomb correlation of O(2*p*) electrons yields the Mott insulating state, consistently with experiments. For O<sub>2</sub>PtF<sub>6</sub>, we have shown that not only correlation effects of both O(2*p*) and Pt(5*d*) electrons but also the strong SO interaction of the 5*d* states are essential to describe its Mott insulating state.

We have performed electronic structure calculations for the experimental unit cell of O<sub>2</sub>MF<sub>6</sub> (*M* = Sb, Pt) with bcc structure of *Ia*<sub>3</sub>(206) space group.<sup>22</sup> We have employed the full-potential augmented plane wave (FLAPW) band method<sup>23</sup> implemented in the WIEN2K package.<sup>24</sup> We have considered the on-site *U* of both O(2*p*) and Pt(5*d*) electrons in the GGA + *U* (Ref. 25), and the SO interaction effect is included as a second variational procedure in the GGA + SO and the GGA + SO + *U* scheme. The spin direction has chosen to be (001) direction for the consideration of SO interaction. For results below, *U* value was chosen to be 10 eV for both O(2*p*) and Pt(5*d*) states.<sup>26</sup> To allow the orbital polarization of  $\pi_g^*$  states, as was realized in KO<sub>2</sub> superoxide,<sup>5</sup> we have removed all the symmetry operators except inversion symmetry.

Figure 3 shows the calculated density of states (DOS) of O<sub>2</sub>SbF<sub>6</sub> in both the GGA and the GGA + SO + *U* schemes. We have assumed the ferromagnetic state for O<sub>2</sub>SbF<sub>6</sub>. Most valence electrons of Sb are transferred into F, and 4*d*<sup>10</sup> occupied states of Sb<sup>5+</sup> are located ~25 eV below *E<sub>F</sub>*. Hence, only a small amount of Sb states originating from the hybridization with F(2*p*) states exists near *E<sub>F</sub>*. Therefore, O<sub>2</sub>SbF<sub>6</sub> is a typical O(2*p*) molecular solid like KO<sub>2</sub>. The GGA in Fig. 3(a) yields the metallic state for O<sub>2</sub>SbF<sub>6</sub> with

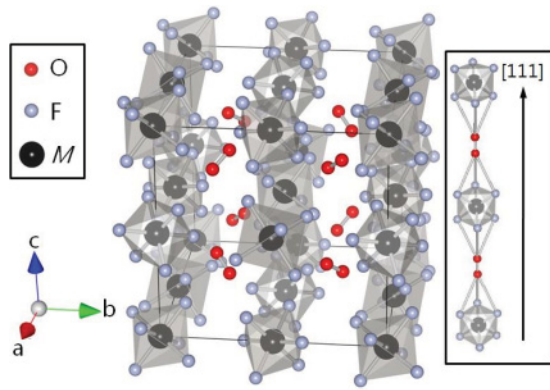


FIG. 1. (Color online) Crystal structure of  $O_2MF_6$  ( $M = \text{Sb}, \text{Pt}$ ) composed of  $O_2^+$  dioxygenyls and  $MF_6^-$  octahedra. There are eight  $O_2^+$  and  $MF_6^-$  ions in a unit cell. (Right inset) Molecular configuration of  $O_2^+$  and  $MF_6^-$  along the [111] direction.

$\pi_g^*$  spin  $\uparrow$  states being located at  $E_F$ . On the other hand, the GGA + SO +  $U$  in Fig. 3(b) considering the correlation effect of  $O(2p)$  electrons yields the correct insulating state by separating the  $\pi_g^*$  states into occupied (lower Hubbard) and unoccupied (upper Hubbard) states with a gap of  $\Delta_H = 2.55$  eV. We have also found that electronic structures in the GGA +  $U$  are almost the same as those in the GGA + SO +  $U$ , implying that the role of the SO interaction in  $O_2\text{SbF}_6$  is minor. Note that, in  $\text{KO}_2$  superoxide, the degenerate  $\pi_g^*$  states tend to be split by coherent tilting of the  $O_2^-$  molecular axes. This mechanism is called “magnetogyration,” which invokes the structural and magnetic transitions concomitantly.<sup>27</sup> Similarly, the degeneracy of the  $\pi_g^*$  states in  $O_2\text{SbF}_6$  is lifted by trigonal CF and hybridization coming from neighboring  $F^-$  ions, which is thought to play a similar role as the conventional Jahn-Teller (JT) effect.<sup>14,15</sup> This feature is revealed in the spin-density (SD) plot in Fig. 5(a), which manifests the directionally polarized  $\pi_g^*$  orbital shape at each  $O_2^+$  site.

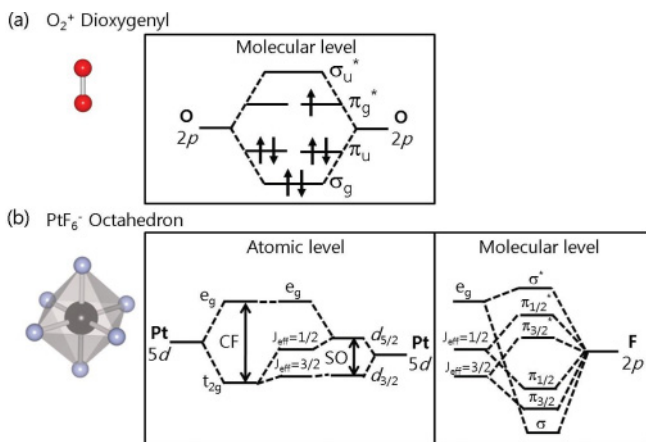


FIG. 2. (Color online) (a) Molecular level of  $O_2^+$  dioxygenyl ion. (b) Schematic local electronic structure of  $\text{PtF}_6^-$  ion.  $\text{Pt}(5d)$  atomic states are split into  $e_g$  and  $J_{\text{eff}} = 1/2, 3/2$  under the octahedral crystal field (CF) with the spin-orbit (SO) interaction. Then  $\text{Pt}(5d)$ - $\text{F}(2p)$  hybridization splits those levels into bonding and antibonding molecular states with  $\pi$  and  $\sigma$  channels.

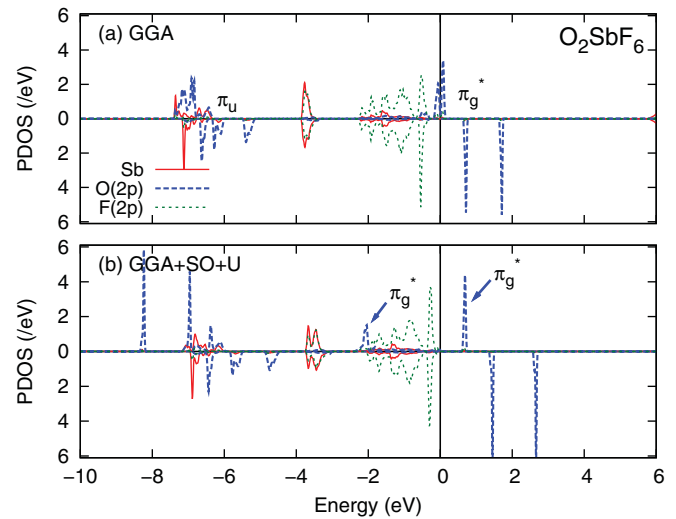


FIG. 3. (Color online) (a) Partial density of states (PDOS) of  $O_2\text{SbF}_6$  in the GGA. The red solid, blue dashed, and green dotted lines denote DOS of Sb,  $O(2p)$ , and  $F(2p)$  states, respectively. (b) PDOS in the GGA + SO +  $U$ . The inclusion of Coulomb correlation yields the separation of  $\pi_g^*$  band into the occupied lower Hubbard and unoccupied upper Hubbard bands, as indicated by blue arrows.  $U$  value was chosen to be 10 eV for  $O(2p)$ .

There was controversy about the existence of SO effects in the  $\pi_g^*$  states of  $O_2MF_6$ . In one group,<sup>14,28</sup>  $g_{\text{eff}}$  factor determined from the magnetic susceptibility and ESR was close to 2 independently of the direction of magnetic field, which reflects the negligible SO effect, while, in the other,<sup>15</sup>  $g_{\text{eff}}$  was reduced a lot along the molecular axis (1.73), which reflects the large orbital moment along that molecular axis. In the present GGA + SO +  $U$  calculation, the orbital magnetic moment is indeed induced along the molecular axis of  $O_2^+$ . However, its magnitude,  $0.02 \mu_B$  per each  $O_2^+$ , is only  $\sim 2\%$  of the spin magnetic moment ( $1.00 \mu_B$ ), which is too small to produce reduced  $g$  factor as reported by Ref. 15. This result implies that the SO interaction is suppressed in  $O_2\text{SbF}_6$  due to the quenched orbital moment of  $O_2^+$ , similarly to the case of low-symmetry structure of  $\text{KO}_2$  (Refs. 5 and 21).

Figure 4 shows the calculated DOS of  $O_2\text{PtF}_6$ . We have assumed the ferrimagnetic ordering between the magnetic moments of  $O_2^+$  and Pt (Ref. 29). Noteworthy is that Mott insulating state is obtained only in the GGA + SO +  $U$  [Fig. 4(b)], in which both the Coulomb correlations of  $O(2p)$  and  $\text{Pt}(5d)$  electrons and the SO interaction are considered. Namely, the GGA, GGA + SO, and GGA +  $U$  schemes without including the SO interaction do not give the correct insulating state of  $O_2\text{PtF}_6$ . The local electronic structure of  $\text{Pt}^{5+}$  in  $O_2\text{PtF}_6$  is close to that of  $\text{Ir}^{4+}$  in  $\text{Sr}_2\text{IrO}_4$ . Both  $\text{Pt}^{5+}$  and  $\text{Ir}^{4+}$  have  $5d^5$  electronic configuration under the octahedral CF with strong SO interaction [see Fig. 2(b)]. Since the CF is stronger than the Hund exchange interaction, they both have the low-spin (LS) states. As shown in Fig. 2(b), the SO interaction splits  $t_{2g}$  states of Pt into  $J_{\text{eff}} = 1/2, 3/2$ , which then hybridize with  $\text{F}(2p)$  states to produce  $\pi_{1/2}$  states at  $E_F$  [see Fig. 4(a)]. Due to the shorter Pt-F bond length ( $\sim 1.88 \text{ \AA}$ ) (Ref. 22) than that of Ir-O ( $\sim 2.00 \text{ \AA}$ ) (Ref. 30), the bands in  $O_2\text{PtF}_6$  are almost like molecular levels. In the GGA + SO in

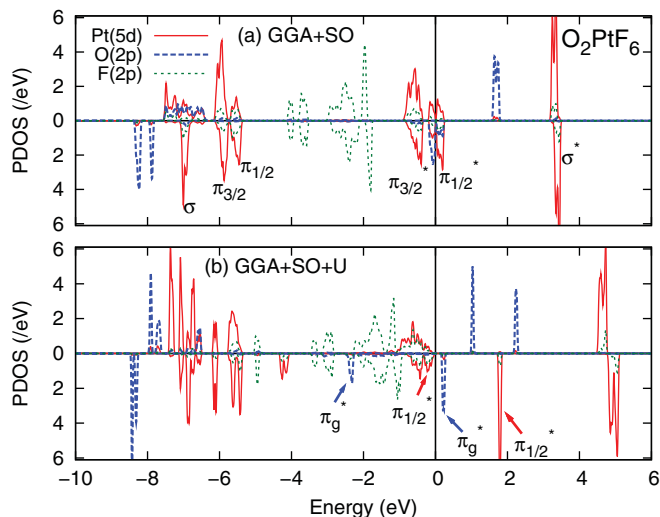


FIG. 4. (Color online) (a) PDOS of  $\text{O}_2\text{PtF}_6$  in the GGA + SO. The red solid, blue dashed, and green dotted lines denote DOS of Pt(5d), O(2p), and F(2p) states, respectively. (b) In GGA + SO + U, inclusion of the Coulomb correlation and the SO interaction yields the separation of (i)  $\pi_g^*$  states of O(2p), as indicated by blue arrows, and (ii)  $\pi_{1/2}^*$  states of Pt(5d), as indicated by red arrows.  $U$  values were chosen to be 10 eV for both O(2p) and Pt(5d).

Fig. 4(a), the SO split  $\pi_{1/2}^*$  states are still degenerate to make  $\text{O}_2\text{PtF}_6$  metallic. The degenerate  $\pi_{1/2}^*$  states become split only after the inclusion of Coulomb interaction of Pt(5d) electrons, as shown in Fig. 4(b). Note that the  $\pi_{1/2}^*$  states are not to be split in the GGA + U even with very large  $U$  value, unless the SO interaction is included.

In general, ions with  $t_{2g}^5$  occupation in the LS state are JT active. It was once reported that reduced  $g_{\text{eff}}$  factor ( $g = 1.86$ ) for the LS state ( $S = 1/2$ ) of  $\text{Pt}^{5+}$  in  $\text{O}_2\text{PtF}_6$  could be explained by the JT effect.<sup>15</sup> The JT distortion, however, has not been detected in  $\text{O}_2\text{PtF}_6$ . The neutron diffraction<sup>31</sup> provided that  $\text{PtF}_6^-$  has a regular octahedron structure. No anomaly in the temperature-dependent magnetic susceptibility<sup>15</sup> for  $\text{O}_2\text{PtF}_6$  also suggests the absence of structural phase transition. Electronic structures in Fig. 4 really verify that the degeneracy of  $t_{2g}$  states is lifted by the SO effect not by the JT effect. The orbital magnetic moment of Pt ion is as much as  $0.52 \mu_B$ , which is comparable to the spin magnetic moment of  $0.60 \mu_B$ . Thus, it is this large orbital magnetic moment of Pt that is responsible for the deviation of the observed  $g_{\text{eff}}$  factor from two. Indeed, the feature of the lifted degeneracy is revealed in the SD plot in Fig. 5(b), which manifests the directionally nonpolarized  $\pi_{1/2}^*$  orbital shape at each  $\text{Pt}^{5+}$  site, in contrast to the directionally polarized  $\pi_g^*$  orbital shape at each  $\text{O}_2^+$  site.

In the case of  $\text{Sr}_2\text{IrO}_4$ , the SO interaction not only splits degenerate  $t_{2g}$  states but also reduces the hybridization with neighboring O(2p) states because of its directionally nonpolarized symmetric nature.<sup>7</sup> Similarly, in  $\text{O}_2\text{PtF}_6$ , Pt(5d)-O(2p) hybridization seems to be reduced a lot by considering the SO interaction. Band structures in Fig. 6 confirm this phenomenon. The blue (red) dot denotes the amount of O(2p) [Pt(5d)] component in the wave function. As shown in Figs. 6(a) and 6(d), without inclusion of the SO interaction

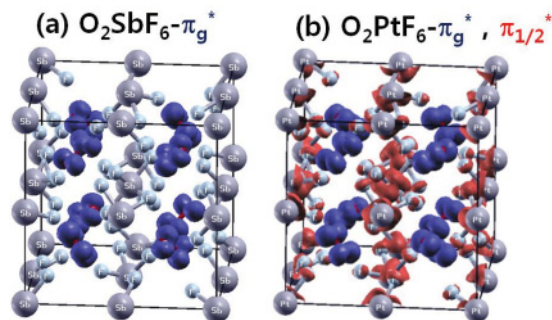


FIG. 5. (Color online) (a) SD plot of  $\text{O}_2\text{SbF}_6$  in the GGA + SO + U. Directionally polarized  $\pi_g^*$  orbitals in blue are manifested. (b) SD plot of  $\text{O}_2\text{PtF}_6$  in the GGA + SO + U. The directionally polarized  $\pi_g^*$  orbitals in blue (dark) and the directionally non-polarized  $\pi_{1/2}^*$  orbitals in red (light) are manifested.

(GGA and GGA + U), bands near  $E_F$  are more dispersive. In contrast, inclusion of the SO interaction in the GGA + SO and GGA + SO + U reduces (i) the band dispersion, (ii) the overlap between O(2p)-Pt(5d) states, and (iii) the direction dependence of O(2p) and Pt(5d) components, as clearly seen in Figs. 6(b) and 6(c). The SO split  $\pi_{1/2}^*$  state in Fig. 6(b) has a narrow band width of  $W = 0.44$  eV, which is much smaller

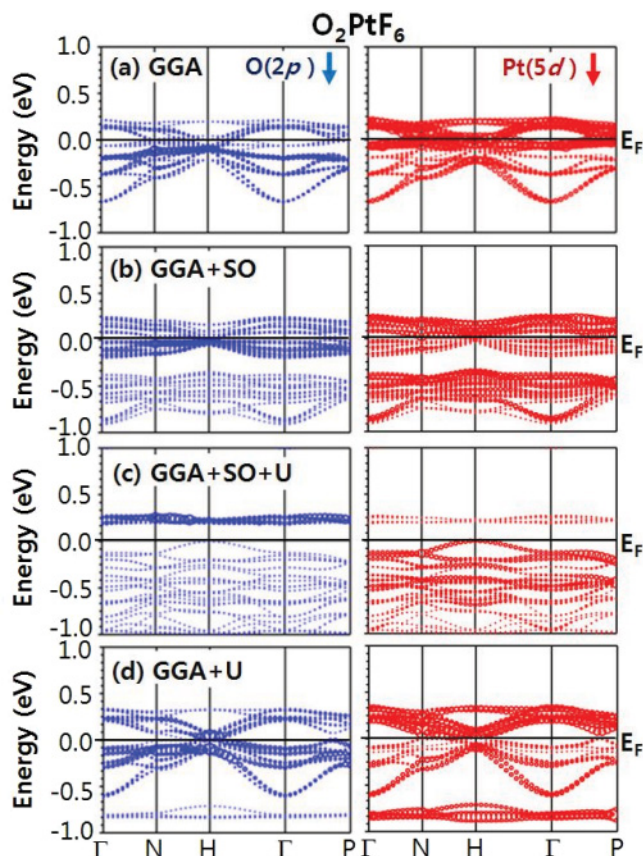


FIG. 6. (Color online) (a) Spin  $\downarrow$  band structures of  $\text{O}_2\text{PtF}_6$  in the GGA. The size of blue [red] dot denotes the amount of O(2p) [Pt(5d)] component in the wave function. (b) The same as (a) in the GGA + SO. (c) The same as (a) in the GGA + SO + U. (d) The same as (a) in the GGA + U.

than that of the original antibonding  $\pi$  states ( $W = 0.84$  eV) in Fig. 6(a). Therefore, the SO interaction plays an important role in realizing the Mott insulating state of  $\text{O}_2\text{PtF}_6$ , as in the case of  $\text{Sr}_2\text{IrO}_4$ .

In conclusion, we have demonstrated that dioxygenyl magnet  $\text{O}_2\text{PtF}_6$  is the first  $2p$  electron Mott insulator induced by combined effects of the Coulomb correlation and the SO interaction. For  $\text{O}_2\text{SbF}_6$ , a typical  $2p$  molecular solid, we have shown that the Coulomb correlation of  $\text{O}(2p)$  electrons drives the Mott insulating state. The SO interaction in dioxygenyl  $\text{O}_2^+$  in  $\text{O}_2\text{SbF}_6$  is suppressed by the strong CF of neighboring  $\text{F}^-$  ions, as was corroborated by the quenched orbital moment of  $\text{O}_2^+$ . For  $\text{O}_2\text{PtF}_6$ , the Mott insulating state is obtained

by considering both the Coulomb correlation of  $\text{O}(2p)$  and  $\text{Pt}(5d)$  electrons and the SO interaction of  $\text{Pt}(5d)$  states. The role of the SO interaction in  $\text{O}_2\text{PtF}_6$  is similar to the case of  $\text{Sr}_2\text{IrO}_4$ , which implies that  $\text{O}_2\text{PtF}_6$  is also a typical SO-induced Mott system with  $J_{\text{eff}} = 1/2$ . The proposed aspects of strong SO interaction in  $\text{O}_2\text{PtF}_6$  remain to be confirmed by further experiments: (i) large orbital moment of Pt ion, (ii) absence of the JT distortion of  $\text{PtF}_6$  octahedron at low temperature.

This work was supported by the NRF (Grant No. 2009-0079947). Helpful discussions with Beom Hyun Kim are greatly appreciated.

- 
- <sup>1</sup>M. Imada, A. Fujimori, and Y. Tokura, *Rev. Mod. Phys.* **70**, 1039 (1998).
- <sup>2</sup>K. I. Kugel and D. I. Khomskii, *Sov. Phys. JETP* **37**, 725 (1973).
- <sup>3</sup>B. H. Kim, H. Choi, and B. I. Min, *New J. Phys.* **12**, 073023 (2010).
- <sup>4</sup>I. V. Solovyev, *New J. Phys.* **10**, 013035 (2008).
- <sup>5</sup>M. Kim, B. H. Kim, H. C. Choi, and B. I. Min, *Phys. Rev. B* **81**, 100409(R) (2010).
- <sup>6</sup>J.-S. Kang, D. H. Kim, J. H. Hwang, J. Baik, H. J. Shin, M. Kim, Y. H. Jeong, and B. I. Min, *Phys. Rev. B* **82**, 193102 (2010).
- <sup>7</sup>B. J. Kim, H. Jin, S. J. Moon, J.-Y. Kim, B.-G. Park, C. S. Leem, Jaejun Yu, T. W. Noh, C. Kim, S.-J. Oh, J.-H. Park, V. Durairaj, G. Cao, and E. Rotenberg, *Phys. Rev. Lett.* **101**, 076402 (2008).
- <sup>8</sup>S. J. Moon, H. Jin, K. W. Kim, W. S. Choi, Y. S. Lee, J. Yu, G. Cao, A. Sumi, H. Funakubo, C. Bernhard, and T. W. Noh, *Phys. Rev. Lett.* **101**, 226402 (2008).
- <sup>9</sup>D. Pesin and L. Balents, *Nat. Phys.* **6**, 376 (2010).
- <sup>10</sup>H. Watanabe, T. Shirakawa, and S. Yunoki, *Phys. Rev. Lett.* **105**, 216410 (2010).
- <sup>11</sup>H. J. Xiang and M.-H. Whangbo, *Phys. Rev. B* **75**, 052407 (2007).
- <sup>12</sup>Guo-Qiang Liu, V. N. Antonov, O. Jepsen, and O. K. Andersen, *Phys. Rev. Lett.* **101**, 026408 (2008).
- <sup>13</sup>S. Sarkar, M. DeRaychaudhury, I. Dasgupta, and T. Saha-Dasgupta, *Phys. Rev. B* **80**, 201101(R) (2009).
- <sup>14</sup>A. Grill, M. Schieber, and J. Shamir, *Phys. Rev. Lett.* **25**, 747 (1970).
- <sup>15</sup>F. J. Disalvo, W. E. Falconer, R. S. Hutton, A. Rodriguez, and J. V. Waszczak, *J. Chem. Phys.* **62**, 2575 (1975).
- <sup>16</sup>P. Botkovitz, G. M. Lucier, R. P. Rao, and N. Bartlett, *Acta Chim. Slov.* **46**, 141 (1999).
- <sup>17</sup>J. J. Attema, G. A. de Wijs, G. R. Blake, and R. A. de Groot, *J. Am. Chem. Soc.* **127**, 16325 (2005).
- <sup>18</sup>R. Kováčik and C. Ederer, *Phys. Rev. B* **80**, 140411(R) (2009).
- <sup>19</sup>J. Winterlik, G. H. Fecher, C. A. Jenkins, C. Felser, C. Mühle, K. Doll, M. Jansen, L. M. Sandratskii, and J. Kübler, *Phys. Rev. Lett.* **102**, 016401 (2009).
- <sup>20</sup>E. R. Ylvisaker, R. R. P. Singh, and W. E. Pickett, *Phys. Rev. B* **81**, 180405(R) (2010).
- <sup>21</sup>A. K. Nandy, P. Mahadevan, P. Sen, and D. D. Sarma, *Phys. Rev. Lett.* **105**, 056403 (2010).
- <sup>22</sup>O. Graudejus and B. G. Müller, *Z. Anorg. Allg. Chem.* **622**, 1076 (1996).
- <sup>23</sup>M. Weinert, E. Wimmer, and A. J. Freeman, *Phys. Rev. B* **26**, 4571 (1982).
- <sup>24</sup>P. Blaha, K. Schwarz, G. K. H. Madsen, D. Kvasnicka, and J. Luitz, WIEN2K (Karlheinz Schwarz, Technische Universität Wien, Austria, 2001).
- <sup>25</sup>V. I. Anisimov, I. V. Solovyev, M. A. Korotin, M. T. Czyzyk, and G. A. Sawatzky, *Phys. Rev. B* **48**, 16929 (1993).
- <sup>26</sup>We have checked that electronic structures are consistent for  $U$  values of 7–12 eV for  $\text{O } 2p$  and  $\text{Pt } 5d$  electrons. The employed  $U$  value of 10 eV would be screened by the intramolecular hybridization in  $\text{O}_2^+$  or  $\text{PtF}_6^-$  (Ref. 4), as displayed in the smaller energy separation between occupied and unoccupied states of  $\text{O}(2p)$  ( $\Delta_H = 2.55$  eV) or  $\text{Pt}(5d)$  ( $\Delta_H = 1.70$  eV) in Fig. 4(b). The screening by the intramolecular hybridization has also been confirmed experimentally in Ref. 6 for  $\text{KO}_2$ .
- <sup>27</sup>W. Känzig and M. Labhart, *J. Phys. (Paris)* **37**, C7-39 (1976).
- <sup>28</sup>J. Shamir and J. Binenboym, *Inorg. Chim. Acta* **2**, 37 (1968).
- <sup>29</sup>In the GGA + SO and the GGA + SO +  $U$ , the ferrimagnetic (Fi) state is more stable than the ferromagnetic (F) state, while, in the GGA, the F state is more stable than the Fi state.
- <sup>30</sup>T. Shimura, Y. Inaguma, T. Nakamura, M. Itoh, and Y. Morii, *Phys. Rev. B* **52**, 9143 (1995).
- <sup>31</sup>J. A. Ibers and W. C. Hamilton, *J. Chem. Phys.* **44**, 1748 (1966).